EPiC Series in Health Sciences
Volume 7, 2024, Pages 160–166
Proceedings of The 24th Annual Meeting of the International Society for Computer Assisted Orthopaedic Surgery

A validated, patient-specific, muscle mapping model of the shoulder

Blake McCall[1], Geoff Smith[1,2]
[1] University of New South Wales, Sydney, Australia
[2] Department of Orthopaedics, St George Hospital, Sydney, Australia

b.mccall@unsw.edu.au, gcssmith@icloud.com

1 Introduction

Shoulder instability, rotator-cuff tears and osteoarthritis are common, with their aetiology and/or pathogenesis relating to the biomechanics of the rotator cuff and deltoid [1, 2]. A better understanding of internal biomechanical conditions could help improve our understanding of these pathologies.

Patient-specific computational models offer a cost-effective tool to help inform clinicians on the most appropriate treatment strategy for that patient; identify the preferred off-the-shelf implants; or help with the design of patient-specific implants. So far, computational models have led to advances in our understanding of shoulder implant behaviour [3], surgical planning [4] and rehabilitation [5].

The accuracy of computational modelling in predicting musculoskeletal biomechanics, relies on their ability to predict realistic muscle paths [6-8]. Previously, models combining muscle line segment and finite element (FE) approaches have been developed, Favre et al and Elwell et al present similar methods relying upon FE contact detection features to wrap the line segments around the underlying geometry [9, 10]. Although more efficient than 3D volumetric models, they still require significantly more computation time than traditional line segment models. Furthermore, they rely upon access to commercial FE software packages with adequate contact detection features. Thus, current muscle path modelling approaches struggle to find a balance between efficiency and accuracy.

The aim of this study was to develop a patient-specific, line-segment muscle mapping model capable of predicting muscle paths during abduction, flexion, and axial rotation. Muscle moment arms and lines of action were compared against ex vivo cadaveric data [11, 12] and muscle lengths and excursions were compared against in vivo MRI [13] and ex vivo cadaveric measurements [14].

2 Methods

Triangular mesh was generated from segmentations of an anonymized male (75 years old, 23 BMI). The locations of the origin and insertion of each muscle was based off previously reported data [15]. A 'convex hull' wrapping algorithm was developed to determine muscle paths and compute muscle lengths, moment arms and line of action for each muscle fibre. The algorithm was applied at static angles of coronal plane glenohumeral abduction, sagittal plane flexion and axial rotation at neutral elevation ranging from 0-90° with 2.5° intervals.

A mesh convergence study investigated the effect of surface mesh edge length on maximum moment arm and computational time for 0-90° abduction. Muscle fibre length was calculated at 0° abduction and compared against published experimental data measured from MR imaging [13] and cadaveric tissue [16]. Muscle moment arms were then calculated using the tendon excursion method [17]. Predicted moment arms were validated qualitatively against cadaveric data [11], by comparing moment arm graphs for each muscle subgroup during flexion and abduction Figure 1.

The 'line of action' angle of each muscle fibre was computed [12].

To better illustrate each muscle subgroups potential to contribute to anterior/posterior and superior/inferior glenohumeral joint stability, average stability ratios were calculated Figure 2.

3 Results

Predicted muscle lengths were within one standard deviation of in vivo MRI measurements reported by Holzbaur et al [13].

Our model correctly predicted abductor/adductor action of all multipennate muscles during abduction when compared to Ackland et al [11]. Our model demonstrated the anterior and middle deltoid to be the largest abductors (30.74 mm & 31.44 mm respectively) and the supraspinatus the largest flexor (47.97 mm). In contrast, the largest adductor was the subscapularis (12.45 mm) and the largest extensor the posterior deltoid (38.64 mm) which agreed with the maximum moment arms reported in the literature Figure 1

Our model correctly predicted the anterior/posterior and inferior/superior stabilising potential of most muscle subgroups. During abduction and flexion, the supraspinatus was the most significant potential joint stabilizer while the deltoid muscles were the largest potential superior destabilisers and the rotator cuff muscles were the most prominent inferior destabilisers, in agreement with the cadaveric data Figure 2

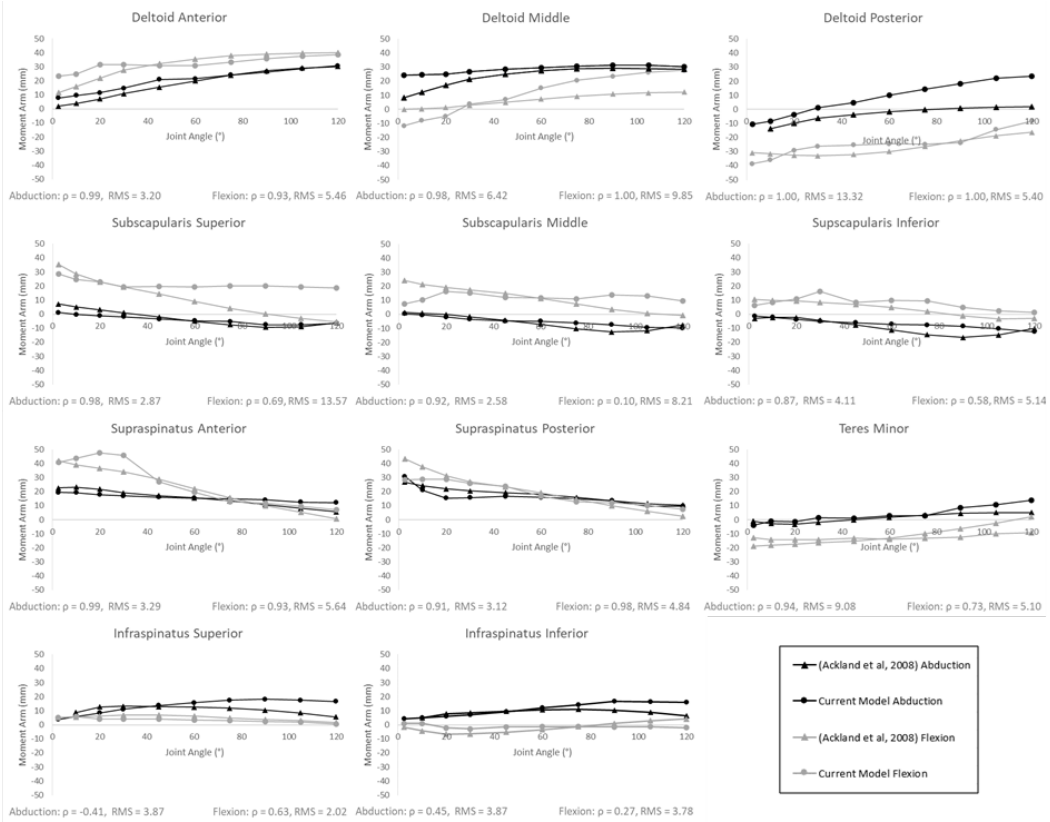

Figure 1: Average muscle moment arms for each muscle subgroup compared against experimental in vivo data. Circular nodes represent predicted moment arms for current model and triangular nodes represent in vivo moment arm values. Black lines represent coronal plane abduction and grey lines represent sagittal plane flexion. Positive values indicate either abductor or flexion muscle action, while negative values indicate adductor or extension action. Average spearman's rank correlation coefficient (ρ) as well as root mean square error (RMS) between current model and in vivo data for 0-90° joint angle is shown for each muscle subgroup.

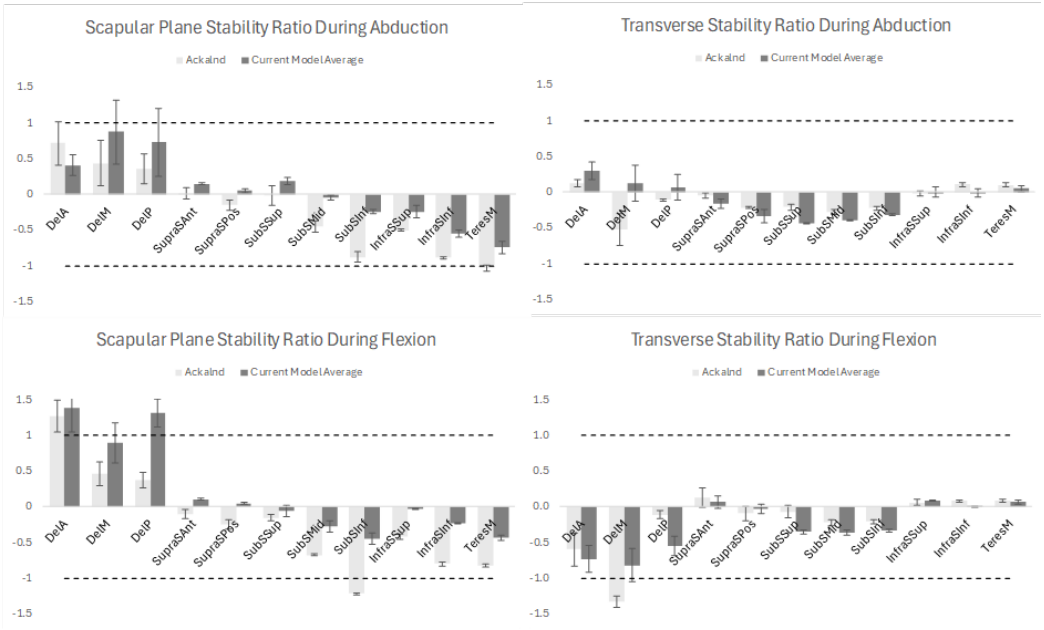

Figure 2: Averaged superior and anterior stability ratios of muscles crossing the glenohumeral joint during abduction and flexion for current model compared against cadaveric data. For stability ratios in the scapular plane, positive values indicate a muscle with an average a superior shear component while negative values indicte an average inferior shear component. For stability ratios in the transverse plane, postive values indicate a muscle with an average anterior shear component while negatvie values indicate an average posterior shear component. A muscle with a stability ratio of > 1 was considered a destabiliser, as the shear component of its line of action was larger than the compressive component. Conversely, a muscle with a stability ratio of < 1 was considered a stabilizer, as the shear component of its line of action was smaller than the compressive component.

4 Discussion

Our model improves upon existing models by considering patient-specific anatomy without the need for FE contact detection, requiring only two simple inputs, surface mesh node coordinates, and origin/insertion coordinates, as a result the model is highly computationally efficient. Our model is also capable of mapping multiple fibres for each muscle, allowing for muscles to be divided into multi-pennate subgroups. EMG studies have shown the rotator cuff and deltoid to have functionally independent sub-regions [18] and representing these sub-regions of muscles by single lines-of-action does not yield accurate estimates of muscle moment arms and joint torques [19]. Previous studies combined the teres minor and superior/inferior subscapularis as a single muscle [20-22]. However, the current study demonstrated these muscles to have distinct torque producing potential in both abduction and flexion. During abduction, the teres minor acted as both an adductor and abductor whereas the infraspinatus produced solely abduction action. Furthermore, during flexion the infraspinatus superior demonstrated solely flexor action while the infraspinatus inferior demonstrated mainly extensor action.

Differences in moment arms and line of action between our model and Ackland et al, may be associated to methodological differences. A paper investigated the effect of varying the muscle insertion sites, demonstrated that moment arms can vary up to 20mm during abduction, possibly reversing the muscle role from abductor to adductor and vice versa [23]. Furthermore, the current study used the anatomy of a 75-year-old male, whereas Ackland et al used averaged data from 8 cadavers

(mean age of 87 years old). Differences in patient-specific anatomy, specifically humeral head size also has an impact on muscle moment and since humeral head data from Ackland et al was inaccessible, normalisation of the results could not be performed.

However, there are several limitations to this model. Firstly, the muscle wrapping algorithm did not represent any soft tissues within the shoulder girdle. Second, motion was applied to the humerus only, limiting all other degrees of freedom and therefore not accounting for scapulothoracic motion. Finally, only muscle paths which wrapped closest to the bony geometry were represented without capturing entire muscle thickness.

The model could easily be adapted to include total shoulder arthroplasty prosthesis, in which case, changes in moment arms and muscle elongation following arthroplasty can be predicted and help clinicians identify the optimal implant configuration and positioning.

5 References

1. Gerber, C., S.H. Wirth, and M. Farshad, Treatment options for massive rotator cuff tears. J Shoulder Elbow Surg, 2011. 20(2 Suppl): p. S20-9.

2. Bigliani, L.U., et al., Glenohumeral stability. Biomechanical properties of passive and active stabilizers. Clin Orthop Relat Res, 1996(330): p. 13-30.

3. Kontaxis, A. and G.R. Johnson, The biomechanics of reverse anatomy shoulder replacement--a modelling study. Clin Biomech (Bristol, Avon), 2009. 24(3): p. 254-60.

4. Magermans, D.J., et al., Requirements for upper extremity motions during activities of daily living. Clin Biomech (Bristol, Avon), 2005. 20(6): p. 591-9.

5. Saul, K.R., et al., Postural dependence of passive tension in the supraspinatus following rotator cuff repair: a simulation analysis. Clin Biomech (Bristol, Avon), 2011. 26(8): p. 804-10.

6. van der Helm, F.C., Analysis of the kinematic and dynamic behavior of the shoulder mechanism. J Biomech, 1994. 27(5): p. 527-50.

7. Charlton, I.W. and G.R. Johnson, Application of spherical and cylindrical wrapping algorithms in a musculoskeletal model of the upper limb. J Biomech, 2001. 34(9): p. 1209-16.

8. Garner, B.A. and M.G. Pandy, Musculoskeletal model of the upper limb based on the visible human male dataset. Comput Methods Biomech Biomed Engin, 2001. 4(2): p. 93-126.

9. Elwell, J.A., G.S. Athwal, and R. Willing, Development and validation of a muscle wrapping model applied to intact and reverse total shoulder arthroplasty shoulders. J Orthop Res, 2018. 36(12): p. 3308-3317.

10. Favre, P., C. Gerber, and J.G. Snedeker, Automated muscle wrapping using finite element contact detection. J Biomech, 2010. 43(10): p. 1931-40.

11. Ackland, D.C., et al., Moment arms of the muscles crossing the anatomical shoulder. J Anat, 2008. 213(4): p. 383-90.

12. Ackland, D.C. and M.G. Pandy, Lines of action and stabilizing potential of the shoulder musculature. J Anat, 2009. 215(2): p. 184-97.

13. Holzbaur, K.R.S., et al., Upper limb muscle volumes in adult subjects. Journal of Biomechanics, 2007. 40(4): p. 742-749.

14. Labib, M., et al., A Biomechanical Analysis of Shoulder Muscle Excursions During Abduction, After the Treatment of Massive Irreparable Rotator Cuff Tears Using Superior Capsular Reconstruction (SCR), Bursal Acromial Reconstruction (BAR), and SCR with BAR. Journal of Shoulder and Elbow Arthroplasty, 2022. 6: p. 24715492221109001.

15. Johnson, G.R., et al., Modelling the muscles of the scapula morphometric and coordinate data and functional implications. J Biomech, 1996. 29(8): p. 1039-51.

16. Langenderfer, J., et al., Musculoskeletal parameters of muscles crossing the shoulder and elbow and the effect of sarcomere length sample size on estimation of optimal muscle length. Clinical Biomechanics, 2004. 19(7): p. 664-670.

17. An, K., et al., Determination of muscle orientations and moment arms. Journal of biomechanical engineering, 1984. 106(3): p. 280-282.

18. Laursen, B., et al., A model predicting individual shoulder muscle forces based on relationship between electromyographic and 3D external forces in static position. Journal of Biomechanics, 1998. 31(8): p. 731-739.

19. Van der Helm, F.C. and R. Veenbaas, Modelling the mechanical effect of muscles with large attachment sites: application to the shoulder mechanism. J Biomech, 1991. 24(12): p. 1151-63.

20. McMahon, P.J., et al., Shoulder muscle forces and tendon excursions during glenohumeral abduction in the scapular plane. Journal of shoulder and elbow surgery, 1995. 4(3): p. 199-208.

21. Apreleva, M., et al., A dynamic analysis of glenohumeral motion after simulated capsulolabral injury. A cadaver model. JBJS, 1998. 80(4): p. 474-80.

22. Kedgley, A.E., et al., The effect of muscle loading on the kinematics of in vitro glenohumeral abduction. Journal of biomechanics, 2007. 40(13): p. 2953-2960.

23. Hoffmann, M., et al., Influence of glenohumeral joint muscle insertion on moment arms using a finite element model. Comput Methods Biomech Biomed Engin, 2020. 23(14): p. 1117-1126.